THE CLINOPYROXENES OF A MONZONITIC COMPLEX AT MOUNT DROMEDARY, NEW SOUTH WALES

R. S. Boesen, *Department of Geophysics, Australian National University, Canberra, A.C.T., Australia.*

Abstract

Mt. Dromedary is located on the south coast of New South Wales, about eighty-five miles south-east of Canberra. The monzonitic complex crops out over twenty-five square miles and consists chiefly of several small stock-like intrusions. Strong differentiation has produced a rock series which extends from ultramafic to peralkaline types. The pyroxene assemblage consists entirely of a lime-rich monoclinic variety; sub-calcic augite, pigeonite and orthopyroxene have not been observed. Thirteen clinopyroxenes, separated from the more important members of the complex, have been chemically analyzed and the optical properties determined. On the conventional atomic Ca-Mg-Fe diagram, the plots of the analyses are scattered along the salite-augite boundary and trend from $Ca_{46}Mg_{41}Fe_{13}$ to $Ca_{43}Mg_{32}Fe_{25}$. This compares very closely with the differentiation trend proposed by Wilkinson (1956) for the clinopyroxenes of alkali basalt magma. The pyroxenes invariably show a zonal structure, and this is described in detail.

Introduction

In this paper, "tholeiite" is meant to indicate the oversaturated rather than the undersaturated types unless otherwise specified, whereas "alkali basalt" refers to alkali olivine-basalt (Tilley, 1950) as described by Wilkinson (1956, 1958).

Trends of pyroxene composition have been studied in strongly fractionated single intrusions of tholeiite and alkali basalt magma. The tholeiitic trend is shown in the Skaergaard intrusion (Muir, 1951; Brown, 1957; Brown and Vincent, 1963) and the Tasmanian dolerites (Edwards, 1942; McDougall, 1961), and the alkali basalt trend has been described from the Garbh Eilean sill (Murray, 1954) and the Black Jack sill (Wilkinson, 1957).

The monzonitic complex at Mt. Dromedary has been emplaced in a previously stabilized orogenic belt. Chemically it is characterized by relatively high figures for potash, alumina and lime. The alkali-lime index (Peacock, 1931) is about 53 for the whole complex, and about 50 for the alkali-rich rocks.

This paper contains a brief account of the petrography of some members of the complex, and the detailed results of optical and chemical studies of their clinopyroxenes. These are compared with pyroxenes from other alkaline complexes, and the relationship of the trend from Mt. Dromedary to that established for rocks of alkali basalt parentage is discussed.

The Monzonitic Complex

The monzonitic complex at Mt. Dromedary consists of a number of stock-like bodies of probable Middle Cretaceous age (Evernden and Richards, 1962) intruded into tightly folded argillaceous and cherty beds "regarded tentatively as of middle or upper Cambrian age" (Brown, 1933, p. 335).

Mt. Dromedary is the eroded remnant of a composite igneous intrusion. The older of the two members is composed of monzonite and has a nearly circular outcrop about $4\frac{1}{2}$ miles in diameter. The younger member is a banatite with a strongly porphyritic marginal zone; its outcrop is also nearly circular, with a diameter of 3 miles. The banatite crops out within, and concentric with, the older monzonite, cropping out from the summit (in plan, approximately the common center of the intrusions) to near the foot of the mountain, where the porphyritic marginal phase intrudes the monzonite of the lower slopes. One half of the total outcrop of the complex is taken up by banatite, one quarter by monzonite; the remaining quarter consists of small outcrops of rocks with monzonitic affinities, minor amounts of volcanic rock, and a large number of narrow dikes. Several bodies of pyroxenite are closely associated in the field with the more felsic intrusives and are thought to be related to them.

The satellitic intrusions crop out in the country rock within about 2 miles of the outer contact of the monzonite at Mt. Dromedary, around the southern aspect of the mountain.

Petrography

A petrographic description of the complex was given in an earlier study of the district (Brown, 1930) and will be revised by the present author elsewhere; consequently only a brief outline of the relevant rocks is given below.

The numbering of the rock descriptions corresponds to that of their respective pyroxene or pyroxenes which have been analyzed.

(1). *Laminated pyroxenite* (loc. Poole's Point). The rock is dark gray, medium-grained and rather dense, and consists of a repeated alternation of laminae about 1.5 mm thick, one rich in strongly aligned, tabular bytownite grains, the other rich in prismatic clinopyroxene and tabular forsteritic olivine. Ilmenite-magnetite intergrowths are common, and there are small amounts of magnesian biotite and stumpy euhedra of apatite. This writer believes that the lamination is analogous to the inch-scale layering described by Hess (1960) in the Stillwater igneous complex. However, the laminated rock is clearly not *in situ,* as it is enclosed by a coarser, more massive pyroxenite, very much like (6) below.

(2). *Hybrid dike* (loc. Poole's Point). Occurs similarly to (3) below but has a rather lighter color in hand specimen. The rock is weakly porphyritic in clinopyroxene and has only weak mineral orientation. The groundmass is composed of abundant, very ragged grains of olive-brown biotite, anhedral plates of strongly zoned plagioclase ($An_{75}-An_{49}$), small clinopyroxene grains and a host of tiny acicular apatite crystals.

(3). *Basic dike* (loc. Poole's Point). This narrow dike intrudes the massive pyroxenite mentioned above. The dike-rock is dark gray, medium- to fine-grained, and porphyritic in clinopyroxene. The groundmass has a marked fluxion structure and is composed of bytownite, clinopyroxene optically identical with the phenocrysts, tabular grains of forsteritic olivine, abundant ilmenite-magnetite grains, titaniferous, magnesian biotite flakes, and numerous small apatite needles.

(4). *Monzonite* (loc. Mt. Dromedary). A dark gray, coarse-grained, rather micaceous rock, composed of zoned plagioclase grains ($An_{55}-An_{36}$) set in plates of alkali feldspar, and variable amounts of biotite, hornblende, subhedral pyroxene (which may or may not be associated with the other mafic minerals), opaques and trace amounts of quartz. The pyroxene commonly makes up 10 vol. per cent of the rock.

(5). *Banatite* (loc. Mt. Dromedary). A pink or yellow, coarsely porphyritic rock, made up of abundant, well-formed alkali feldspar phenocrysts set in a medium-grained matrix of alkali feldspar, zoned plagioclase ($An_{30}-An_{20}$), ragged grains of biotite and hornblende (either of which may or may not enclose the few, rounded grains of pyroxene), a small amount of quartz, and opaques.

(6). *Pyroxenite* (loc. 3 miles east of Mt. Dromedary Trig). As mentioned above, this rock closely resembles the massive pyroxenite at Poole's Point, $2\frac{1}{2}$ miles to the east. Both this exposure and (7) are surrounded on three sides by nepheline monzonite (10, below). The rock is very dark green, coarse grained and dense; it is composed very largely of pale green, equant pyroxene subhedra, interstitial labradorite-bytownite, numerous small grains of magnetite-ilmenite, and equant subhedra of apatite.

(7). *Garnet-pyroxene rock* (loc. 3 miles east of Mt. Dromedary Trig). This assemblage has been developed from place to place in the pyroxenitic rocks which are associated in the field with the nepheline monzonite. The andraditic garnet has formed chiefly at the expense of pyroxene and, to a lesser extent, plagioclase of the original pyroxenite. The proportions of

the constituents vary widely over very short distances, but garnet+pyroxene makes up about 70 vol. per cent, and intermediate plagioclase+minor alkali feldspar about 20 vol. per cent; the remainder consists of apatite, opaques, sphene and epidote. The mid-green pyroxene has been extensively replaced by the other minerals and has a poikiloblastic form.

(8). *Shonkinite* (loc. 2 miles south-east of Mt. Dromedary Trig). The rock is medium-grained, dark green-gray and micaceous. It contains euhedra of pale green pyroxene set in plates of alkali feldspar with variable amounts of biotite, olivine, nepheline, magnetite-ilmenite intergrowths and apatite.

(9A, 9B). *"Ijolite"* (loc. 2 miles south of Mt. Dromedary Trig). Hand specimens resemble medium-grained diorite, but in thin section the rock has a most unusual appearance. The felsic minerals include alkali feldspar, strongly zoned plagioclase, and nepheline; the mafics include very dark green hornblende subhedra, very minor biotite flakes, pyroxene euhedra with pale yellow-green cores and mid-green rims, and andraditic garnet. Apatite and calcite are common accessories. The grain size and abundance of each mineral species vary erratically. Pyroxene 9A is the core fraction and 9B is the rim fraction.

(10A, 10, 10B). *Nepheline monzonite* (loc. 3 miles east of Mt. Dromedary Trig). This body also shows local variations in the proportions of its minerals. The felsic constituents are alkali feldspar, zoned andesine, and nepheline; the mafics include pyroxene, usually with pale green cores and mid-green borders, dark olive-green hornblende, and yellow-brown biotite. A few small grains of andraditic garnet have been noted, associated with the pyroxene in mafic clots. Pyroxenes 10A and 10B are core and rim fractions respectively, and 10 is the bulk pyroxene.

The form of the clinopyroxenes varies from one rock type to another, according to the particular conditions of crystallization. For example, the pyroxene grains in the laminated pyroxenite are roughly prismatic in form but have nibbled outlines, which, together with other microscopic features, indicate slight recrystallization of the rock. The pyroxene in the massive pyroxenite has almost identical optical properties with those of the laminated pyroxenite, but lacks the recrystallization textures. In the monzonite and banatite the mineral occurs as rounded subhedral grains, at times enclosed by biotite or hornblende. The "ijolite" and shonkinite contain equant euhedra, but the pyroxene of the nepheline monzonite occurs as subhedral grains which are commonly enveloped by the other mafic minerals. The pyroxene textures in the garnet-pyroxene rock are

typically metamorphic, and poikiloblastic plates are common in thin sections.

Determinative Techniques

Considerable difficulty was experienced in the separation of co-existing pyroxene and amphibole, since the range of specific gravity and magnetic properties of the minerals are very similar. Where the pyroxenes are conspicuously zoned, as in the "ijolite" and nepheline monzonite, and intimately associated with hornblende, a portion of the most ferroan fraction was discarded because of hornblende impurities. As a result, the quoted limit of iron enrichment of these pyroxenes may be very slightly in error. For similar reasons the actual composition of the diopsidic fractions of the zoned pyroxenes may be very slightly more magnesian than is stated here.

The optical properties were determined both from crushes of the analyzed material and from appropriately oriented grains picked from thin sections. The β indices were measured using ordinary immersion techniques on (100) parting tablets (Hess, 1949); α and γ were measured on grains giving centered BxA and BxO figures in thin sections. Care was taken to minimize the effect of temperature variations during index determinations, and the index of the matching oil was immediately checked using an Abbé-type refractometer. $Z \wedge c$ was measured on twinned grains (Hess, 1949). 2V was determined conoscopically (following Hallimond, 1950) by rotation from optic axis to optic axis. All determinations were carried out in sodium light. Maximum probable error of the index determinations is considered to be ± 0.002 and that of the optic axial angles, $\pm 0.5°$.

The classical methods of chemical analysis were employed, with the following modifications: colorimetric techniques were used in the determination of total iron, residual silica and chrome; alumina was determined directly after its extraction by ion exchange; and alkalies were determined using the flame photometer. All samples were ground under acetone and dried for four hours at 105° C. to drive off H_2O^-.

Specific gravity was calculated from the loss in weight of a small sample (about 20 mgm) on immersion in toluene. All measurements were made at 20° C.

Optical Properties

The pyroxenes of the undersaturated alkalic rocks show distinct marginal iron enrichment; other pyroxenes are relatively homogeneous and optically very similar. They vary from almost colorless to a pale applegreen, and pleochroism is weak or absent. The cores of the pyroxene grains in the "ijolite" and nepheline monzonite have a yellow tint which

grades rapidly to olive-green at the borders. Pleochroism is moderate, with X = yellow, Y = olive-yellow and Z = olive-green; absorption is X ≤ Y < Z.

The optic axes show inclined dispersion which is distinct in pyroxenes from the pyroxenites, monzonite and banatite, and strong for those from the alkaline rocks. The color fringes are much more pronounced for the
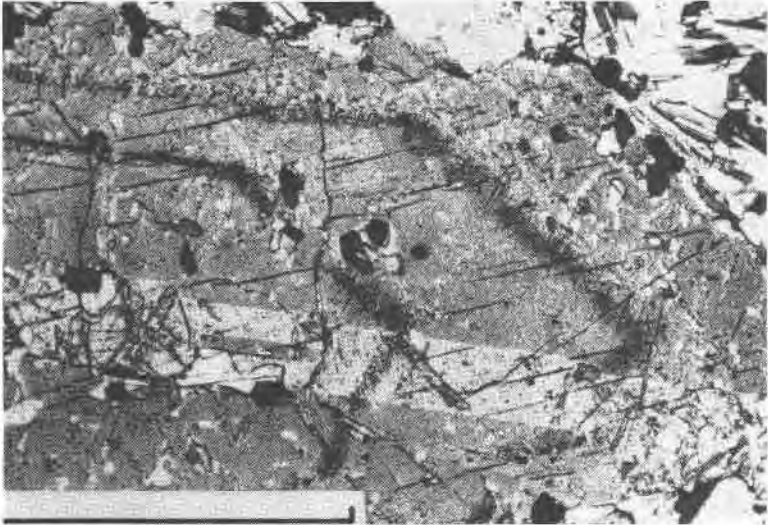

Fig. 1. Twinned pyroxene crystal showing zoning by inclusions. Note abundant plagioclase inclusions in the outer zone and the narrow bands of rutile rods in a sagenitic web. Crossed polars. Scale mark is 1 mm in length.

'B' optic axis emerging near [c], in (001). Twinning, either simple or multiple (Fig. 1), with (100) as the composition plane, is not uncommon.

The optical measurements of the analyzed pyroxenes are listed in Table 2. The refractive indices and 2V are consistently higher than those shown in Hess (1949), but the birefringences are comparable.

The effect of minor elements on the optical properties is not fully understood. Titania apparently causes an increase in the principal refractive indices (Segnit, 1953; Murray, 1954; Wilkinson, 1957; Challis, 1963), and the acmite molecule appears to give higher values for 2V (Yagi, 1953). Although the increase in 2V with increasing soda is apparent in the pyroxenes of this study, their titania content is usually only slightly greater than the 0.4% considered by Hess (1949) in drawing up his determinative curves.

Zoning

The relatively large-scale and irregular core and rim structure of pyroxenes from the "ijolite" and nepheline monzonite has been mentioned above and is not dealt with further. However, the pyroxenes of these rocks show zone phenomena common to the other pyroxenes and are included in the following account.

Except in cases where there is evidence of considerable post-consolidation metamorphism, such as in the garnet-pyroxene rock, the zones are oriented parallel to the crystal faces or, where the texture is such that these are suppressed, parallel to recognizable crystallographic directions. There are three distinct types of zoning, all of which may be developed in the same grain.

In the first type, the zones are picked out by minerals included in the pyroxene, oriented in rows parallel to the crystal outlines. The minerals more commonly found as inclusions are plagioclase, ilmenite-magnetite, apatite, alteration products such as biotite or hornblende, and sagenite (Fig. 1). The zones free of inclusions may or may not lie nearer the crystal margins (Figs. 1, 2).

The second type is characterized by small local variations in color, birefringence and optic orientation of the pyroxene itself, and the zones are relatively broad (Fig. 2).

In exceptional cases these can be seen in thin section without the aid of a microscope. Their average width is about 0.1 mm, with a few reaching 0.5 mm. The difference in optical properties between the zones is slight; the lighter colored portions have slightly lower refractive indices and higher birefringence (up to 0.003) but 2V and $Z \wedge c$ are virtually unchanged throughout the grain. There is a tendency for the sagenite to be developed in the zones of lower birefringence.

The third type is not usually visible except between crossed nicols, and preferably very near an extinction position. Under these conditions the zoning appears as an alternation of very narrow, closely spaced, light and dark striae parallel to the crystal margins. Very commonly it is only the small difference in dispersion between the zones that makes them visible near their extinction position (Figs. 3, 4). The thickness of each zone is of the order of 10^{-4} cm. Hour-glass structure is in some cases associated with this zone type. The zoning closely resembles the fine-scale, oscillatory type common in the plagioclase phenocrysts of andesitic lavas. Examination on the universal stage has shown that, although discontinuities in the zoning are very rare, the adjoining zones grade quickly into one another. There are very few structures analogous to those resulting from resorption during the growth of plagioclase crystals, and the zoning is charac-
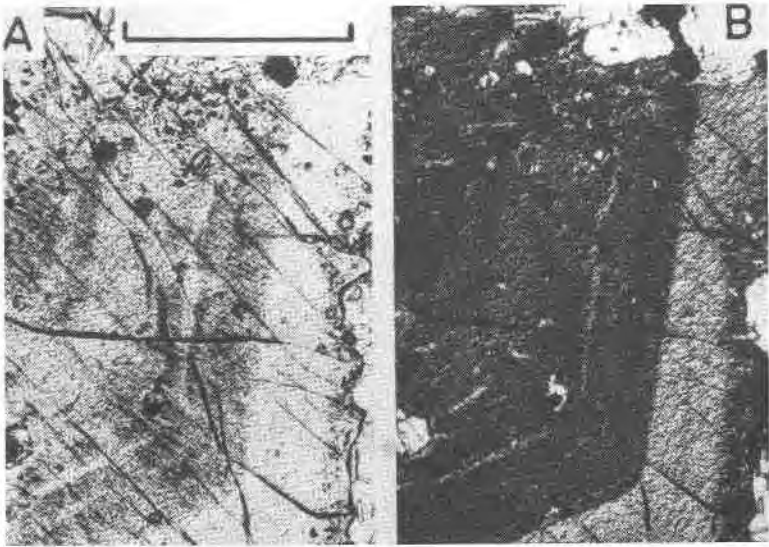
Fig. 2A. Pyroxene grain showing broad outer zone relatively free from inclusions. Abundant tiny rods of rutile (?) are zonally arranged in the inner portion of the grain, and impart a darker color to it. Plane light. Scale mark is 0.2 mm in length.

Fig. 2B. Same, near extinction position. Note difference in extinction angle between the core and the zone free of inclusions.
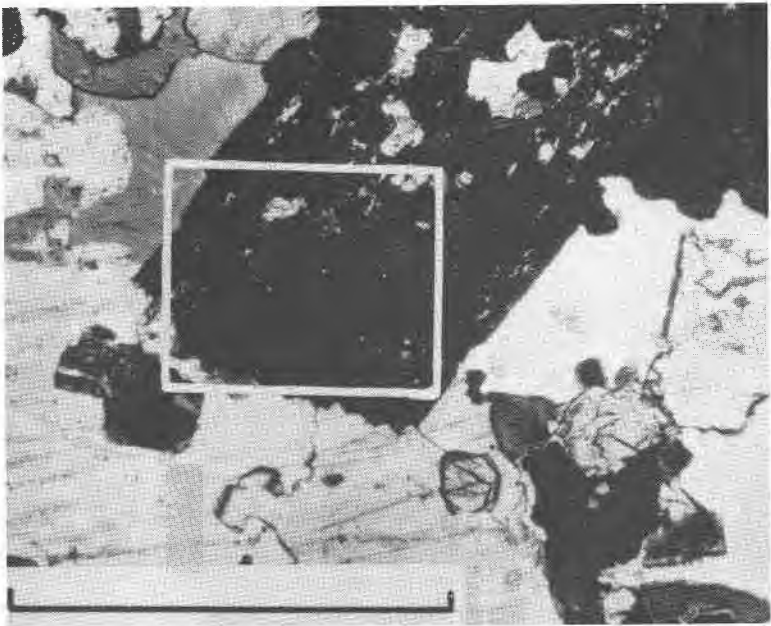

Fig. 3. Shonkinite, with pyroxene crystal very near an extinction position showing lamellar zoning. Area marked is shown in Fig. 4. Convergent light, crossed polars. Scale mark is 1 mm in length.

terized by its regularity. No measurements of 2V, refractive indices, $Z \wedge c$ etc. could be made, because of the very small scale of this zoning. The interference figures obtained on finely-zoned grains were as sharply defined as those obtained from apparently unzoned grains.

Grains of pyroxene showing both types of zoning were examined using an electron micro-analyzer in an attempt to determine the chemical differences between the zones.
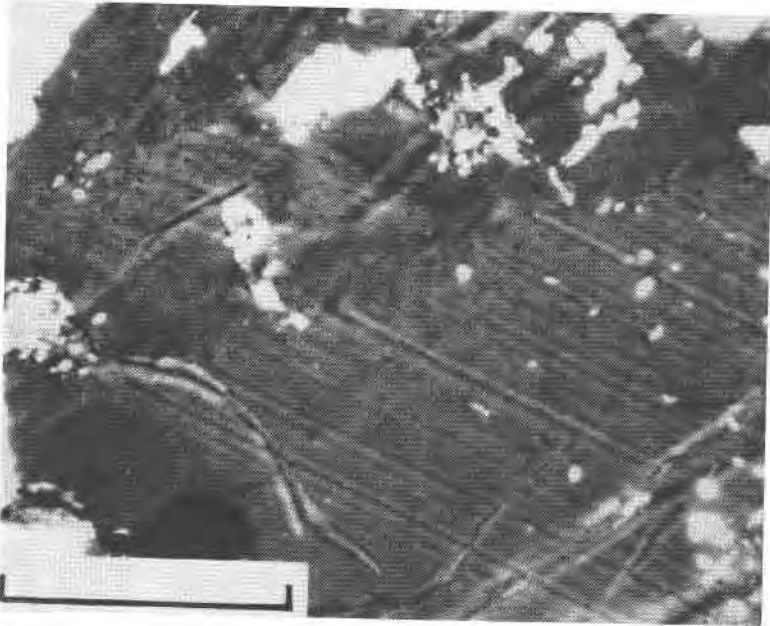

Fig. 4. Detail of pyroxene grain in shonkinite, showing fine lamellar zoning. Convergent light, crossed polars. Scale mark is 0.2 mm in length.

A polished thin section of the shonkinite (Pyroxene 8) was examined microscopically to locate a favorably oriented grain of pyroxene which was relatively free of inclusions, fractures, pits etc., and displayed clearly both the relatively broad and the very fine zones. A detailed, accurate plan of the crystal was prepared (Fig. 5) and a traverse path, normal to the traces of the zones, was chosen. The section was transferred to the electron micro-analyzer and properly oriented by means of the sketch; traverses were then made with the detectors of the instrument adjusted to the different elements before each run so that elemental variations between the zones could be estimated. The results of this approach supported the indications of the optical studies that the variation in chemis-

try was slight. It also became clear that the lamellar zoning was on much too fine a scale to warrant further investigation in this study. Accordingly, the instrument was set to scan repeatedly an area about 0.5 mm square which contained the broader type of zone. The signal from the x-ray detectors was passed to a cathode ray oscilloscope, whose screen was photographed over a period of minutes. In this way a scintillation picture is obtained of the distribution of any particular element in the area
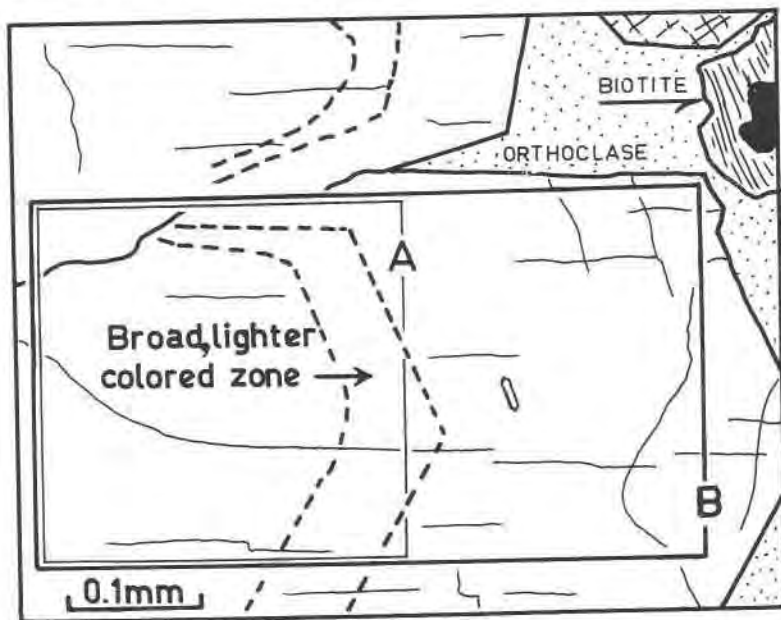

Fig. 5. Diagram of zoned pyroxene studied using the electron microanalyzer. Area marked 'A' is shown in Fig. 6, and area marked 'B' in Fig. 7.

scanned. The relative abundances of an element are roughly proportional to the density of points on the photograph, and if the bulk chemistry is known, as it is in this case, then the absolute variation in the elements can be estimated. Since this method gives a picture of *relative* abundances, a variation of 1% in the content of silica in the pyroxene would be difficult to detect, whereas a 1% variation in the alumina content would be much more apparent.

The best contrast in distribution between the zones was shown by iron and aluminium (Figs. 6, 7), whereas titanium, manganese, chromium and magnesium vary weakly or not at all. The micro-analyzer was not capable of determining sodium, and results with the relatively abundant silicon and calcium were, as expected, noncommittal.
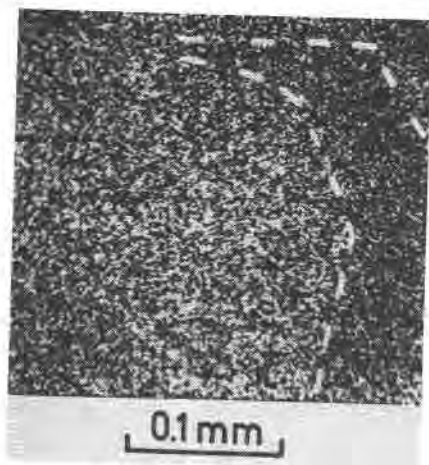
FIG. 6. Scintillation picture showing distribution of Fe over the area marked 'A' in Fig. 5. Broken lines enclose Fe-poor zone.

In summary, the pyroxenes of the monzonitic complex differ texturally, depending on their host rock type, but appear to have very similar optical properties. Very fine, lamellar zoning is characteristic of the pyroxenes, but the structure usually is not visible except between crossed nicols and very near an extinction position. Appreciable compositional zoning occurs only in the pyroxenes from the "ijolite" and nepheline monzonite, both nepheline-bearing rocks. Relatively broad zones of lighter color than the

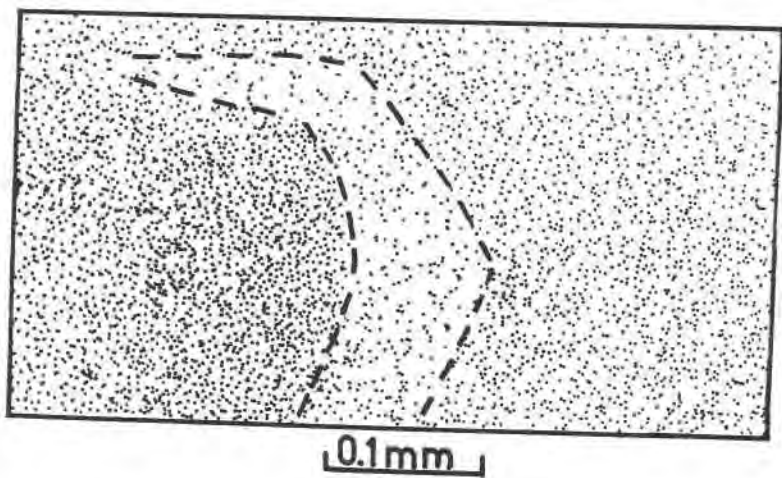FIG. 7. Copy of scintillation pictures showing the distribution of Al over the area marked 'B' in Fig. 5. Broken lines enclose Al-poor zone.

major part of the grain commonly occur within and parallel to the crystal outlines. Preliminary studies of the chemical variations between the zones, using the electron micro-analyzer, indicate that the lighter-colored zones contain considerably less Al and Fe, and approximately constant amounts of Ti, Mn, Cr and possibly Mg. The variation in Si, Na and Ca were not determined.

Pyroxenes more diopsidic than that of the shonkinite (*e.g.* 1, 2 and 3, Table 2) are also lighter colored. Examination of Table 1 shows that the more diopsidic pyroxenes are poorer in Al as well as Fe, so it is very likely that the lighter-colored, broad zones are more diopsidic than the remainder of the grain, and thus represent reverse zoning.

Kuno and Sawatari (1934) described crystals of augite which are zoned in a very similar way to the pyroxenes from the monzonitic complex at Mt. Dromedary. The augites are made up of numerous concentric zones, sometimes of an oscillatory type, often combined with hour-glass structure. The zones are much broader than the lamellar type described in this study, and the authors were able to make detailed measurements of the optical variation between the zones. Their tentative conclusion was that crystallization tended toward decrease in CaO, Fe_2O_3, Al_2O_3 and TiO_2, and increase in MgO. It is interesting to note that these pyroxenes are very pale green, weakly pleochroic, and chemically very similar to those at Mt. Dromedary.

The explanations proposed for reverse and oscillatory zoning in pyroxenes are virtually identical with those put forward to account for similar zoning in plagioclase feldspar, and include intermittent additions of the parent magma, movement of the crystallizing grain within the magma, diffusion between grains of differing composition, and fluctuations in volatile concentration.

Microscopical and field evidence leaves no doubt that the various pyroxenes have crystallized from their host-rocks, except in the case of the altered pyroxenites. It follows that the conditions leading to the zonal growth of the pyroxenes persisted throughout the differentiation and emplacement of the complex.

THE PYROXENE ANALYSES

The formula for clinopyroxene, after Warren and Briscoe (1931), Berman (1937), Hess (1949) and Kuno (1955), is $W_{1-p}(X, Y)_{1+p}Z_2O_6$, where
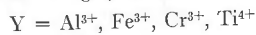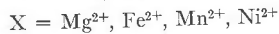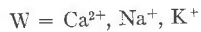
$$W = Ca^{2+}, Na^+, K^+$$
$$X = Mg^{2+}, Fe^{2+}, Mn^{2+}, Ni^{2+}$$
$$Y = Al^{3+}, Fe^{3+}, Cr^{3+}, Ti^{4+}$$
$$Z = Si^{4+}, Al^{3+}, Ti^{4+}\ Fe^{3+}$$

TABLE 1. ANALYSES OF CLINOPYROXENES FROM THE MONZONITIC COMPLEX AT MT. DROMEDARY

	1	2	3	4	5[1]	6	7	8	9A	9B	10A	10	10B
SiO_2	51.15	50.46	50.70	50.59	50.31	50.47	51.80	50.14	50.07	48.60	49.89	49.62	49.66
TiO_2	0.53	0.70	0.48	0.45	0.57	0.73	0.24	0.65	0.63	2.06	0.94	0.82	0.77
Cr_2O_3	0.02	0.08	0.09	0.02	0.06	0.01	0.01	0.05	0.02	0.01	0.02	0.01	0.01
Al_2O_3	3.30	3.73	3.01	2.59	4.11	4.36	1.84	3.90	4.60	4.10	4.95	5.02	5.10
Fe_2O_3	2.40	1.70	2.26	1.78	1.85	2.87	1.82	2.70	2.85	3.25	3.42	3.99	4.27
FeO	5.56	6.60	6.27	9.90	9.22	5.40	7.45	6.56	5.75	11.24	6.16	8.00	9.18
MnO	0.32	0.23	0.28	0.48	0.46	0.15	0.47	0.25	0.20	0.29	0.36	0.46	0.55
MgO	14.08	13.92	14.15	12.58	12.49	13.26	12.38	13.06	13.82	10.22	11.97	10.32	9.26
CaO	22.04	22.00	22.16	20.68	20.53	22.24	22.85	21.88	21.27	19.15	20.95	20.10	18.99
Na_2O	0.55	0.57	0.58	0.62	0.48	0.67	0.61	0.76	0.71	0.95	0.90	1.20	1.57
K_2O	0.02	0.02	0.04	0.08	0.16	0.03	0.03	0.05	0.06	0.10	0.07	0.06	0.16
P_2O_5	0.02	0.02	0.01	0.01	0.04	0.03	0.20	0.04	0.02	nil	0.01	0.01	0.02
H_2O^+	0.11	0.23	0.21	0.29	n.d.	0.14	0.26	0.17	0.17	0.28	0.42	0.60	0.47
Total	100.10	100.26	100.24	100.07	100.23	100.36	99.96	100.21	100.17	100.25	100.15	100.21	100.01

[1] Analyst A. J. Easton; remaining analyses by R. S. Boesen.

1. Pyroxene from laminated feldspathic pyroxenite, Poole's Point. 2. Pyroxene from dike with composition similar to laminated feldspathic pyroxenite, Poole's Point. 3. Pyroxene from hybrid dike, Poole's Point. 4. Pyroxene from coarse monzonite, Central Tilba quarry. 5. Pyroxene from marginal porphyritic phase of banatite, east slope of Mt. Dromedary. 6. Pyroxene from pyroxenite enclosed by nepheline monzonite, 1 mile south-east of Central Tilba. 7. Pyroxene from garnet-pyroxene rock, same locality as (6). 8. Pyroxene from shonkinite, Tilba. 9A, 9B. Core and rim respectively of pyroxene from "ijolite", 2 miles south-west of Tilba Tilba. 10, 10A ,10B. Bulk pyroxene, core and rim pyroxene respectively, from nepheline monzonite, 1½ miles south-east of Central Tilba.

N.B. Analyses grouped in rock types: 1–3 pyroxenites; 4–5 monzonite and banatite; 6–7 altered pyroxenites; 8–10 nepheline-bearing rocks.

The chemical analyses are shown in Table 1, and are recalculated on the basis of six oxygen atoms in Table 3. Although the optical study which preceded the separation and analysis of the pyroxenes gave the first indication that there was probably little variation in their chemistry, such close similarity of the analyses was not anticipated, since silica ranges from 38% in the pyroxenite to more than 62% in the banatite.

Silica remains fairly constant except in the "ijolite" and nepheline monzonite pyroxenes, where it decreases slightly. The figures for silica compare fairly closely with those of calcic tholeiitic clinopyroxenes with a similar degree of iron substitution (Hess, 1949). The Garbh Eilean pyroxenes (Murray, 1954) contain about 1% less silica, and those from the Black Jack sill (Wilkinson, 1957) have 2–3% less.

Titania is relatively low, resembling the amount contained in tholeiitic pyroxenes much more closely than the alkali basalt types. There is no apparent relation between the titania content of the pyroxenes and of their host rocks, nor is there any systematic increase or decrease of this component through the analyses. Indeed, the zoned pyroxenes in the "ijolite" and nepheline monzonite show, respectively, strong marginal enrichment and moderate marginal depletion of titania (Table 1; anal. 9A, 9B, 10A, 10B).

The amount of *alumina* varies considerably, but is more abundant in the pyroxenes of the more alkaline rocks. The alumina figures are rather higher than is usual in tholeiitic clinopyroxenes, but are very similar to those quoted by Murray (1954) for the teschenitic Garbh Eilean sill.

Manganese follows ferrous iron, with the ratio FeO/MnO approximately twenty to one, except for analyses 6 and 9B, which are low in MnO.

The figures for *lime, magnesia* and *ferrous iron* are very similar to those of Murray (1954) and Wilkinson (1957). Ferrous iron enters the pyroxene structure chiefly at the expense of magnesium. The range in values for ferrous iron in these analyses is small compared to that of pyroxenes from tholeiitic rocks showing a similar degree of fractionation (Brown and Vincent, 1963).

Soda is fairly high throughout and increases sharply in the pyroxenes from the nepheline-bearing rocks. The increase in soda is reflected in the increase in the optic axial angle (Table 2). A similar but much stronger trend is recorded by Yagi (1953) for the alkalic rocks of the Morotu district.

Kushiro (1960) and Le Bas (1962) have described, and attempted to account for, the amount and distribution of Si, Al and Ti in calcic igneous clinopyroxenes. Kushiro has shown that when Al is plotted against Si or

TABLE 2. CHEMICAL AND OPTICAL PROPERTIES OF THE CLINOPYROXENES IN TABLE 1

	1	2	3	4	5	6	7	8	9A	9B	10A	10	10B
Composition, atomic per cent													
Ca	46.1	45.9	45.6	43.5	43.9	47.4	48.1	46.3	45.1	43.0	46.5	45.8	44.7
Mg	40.8	40.4	40.6	36.8	37.2	39.2	36.2	38.5	40.8	31.9	36.9	32.8	30.3
Fe[1]	13.1	13.7	13.8	19.7	18.9	13.4	15.7	15.2	14.1	25.1	16.6	21.4	25.0
Specific gravity													
	3.38	3.36	3.36	3.40	—	3.34	3.35	3.36	3.35	3.41	3.36	3.38	3.40
Mean refractive indices													
α	1.694	1.693	1.696	1.696	1.696	1.694	1.695	1.695	1.695	1.702	1.695	—	1.702
β	1.700	1.699	1.701	1.701	1.701	1.700	1.702	1.701	1.703	1.709	1.702	—	1.709
γ	1.721	1.720	1.723	1.723	1.723	1.722	1.724	1.723	1.723	1.730	1.724	—	1.730
Mean $2V_\gamma$	54.0°	54.0°	54.0°	53.5°	53.5°	55.5°	58.5°	54.5°	55.5°	60.0°	56.0°	—	61.5°
$\gamma - \alpha$	0.027	0.027	0.027	0.028	0.027	0.028	0.029	0.028	0.028	0.028	0.029	—	0.028
$Z \wedge c$	40-42°	41-42°	41-43°	43-45°	42-45°	40-43°	43-46°	42-44°	40-43°	45-47°	41-44°	—	44-46°
$\dfrac{FeO + Fe_2O_3}{FeO + Fe_2O_3 + MgO} \times 100:$													
Pyroxene	34.7	37.3	37.6	48.1	47.1	38.4	42.8	41.5	38.4	58.6	44.4	53.8	59.2
Rock	70.5	53.6	49.0	66.6	76.3	67.3	—	58.1	73.8			73.3	

[1] $Fe = Fe^{3+} + Fe^{2+} + Mn^{2+}$.

Specimens numbered as in Table 1.

R. S. BOESEN

TABLE 3. ANALYSES OF TABLE 1 RECALCULATED ON THE BASIS OF SIX OXYGEN ATOMS

		1	2	3	4	5	6	7	8	9A	9B	10A	10	10B
Z	Si	1.900	1.874	1.888	1.912	1.883	1.870	1.950	1.872	1.860	1.851	1.850	1.872	1.874
	Al	0.100	0.126	0.112	0.088	0.117	0.130	0.050	0.128	0.140	0.149	0.150	0.128	0.126
WXY	Al	0.043	0.039	0.022	0.025	0.063	0.062	0.031	0.043	0.061	0.034	0.073	0.084	0.102
	Ti	0.016	0.020	0.013	0.014	0.016	0.020	0.007	0.018	0.018	0.060	0.027	0.023	0.023
	Cr	—	0.004	0.004	—	—	—	—	—	—	—	—	—	—
	Fe^{3+}	0.067	0.049	0.063	0.050	0.054	0.080	0.050	0.076	0.080	0.092	0.095	0.113	0.122
	Fe^{2+}	0.172	0.205	0.195	0.313	0.288	0.167	0.235	0.204	0.179	0.357	0.196	0.245	0.290
	Mn	0.011	0.007	0.009	0.016	0.013	0.004	0.016	0.007	0.007	0.009	0.011	0.014	0.018
	Mg	0.778	0.772	0.785	0.709	0.698	0.733	0.695	0.728	0.766	0.581	0.675	0.581	0.522
	Ca	0.876	0.875	0.884	0.839	0.824	0.884	0.923	0.876	0.848	0.783	0.850	0.812	0.769
	Na	0.040	0.040	0.040	0.045	0.036	0.049	0.045	0.054	0.049	0.069	0.068	0.086	0.114
	K	—	—	—	0.005	0.009	—	—	0.004	0.004	0.005	0.005	0.005	0.009
Z		2.00	2.00	2.00	2.00	2.00	2.00	2.00	2.00	2.00	2.00	2.00	2.00	2.00
WXY		2.00	2.01	2.01	2.02	2.00	2.00	2.00	2.01	2.01	1.99	2.00	1.97	1.97
% Al in Z:		5.0	6.3	5.6	4.4	5.8	6.5	2.5	6.4	7.0	7.5	5.0	6.4	6.3

Specimens numbered as in Table 1.

Ti, the pyroxenes of tholeiitic, feldspathoidal and non-feldspathoidal alkalic rocks fall in three roughly defined fields. A more detailed study along similar lines was made by Le Bas, who effected a clearer distinction between the pyroxenes of the major magma-types by considering only groundmass pyroxene. Le Bas discusses the relation of the amount of aluminium in tetrahedral co-ordination (Al_z) to the total aluminium and to TiO_2, and his plot of Al_z against TiO_2 wt per cent (p. 280) indicates fundamentally different trends, during differentiation, of pyroxenes from the alkaline rocks and from tholeiitic, high-alumina and calc-alkaline rocks.

Comparison of the data from the present study with those of Kushiro and Le Bas shows:

(1) The pyroxenes of the monzonitic complex have relatively small figures for Al_z compared to other pyroxenes with similar proportions of $Ca^{2+}+Na^{+}+K^{+}$, Mg^{2+}, and $Fe^{3+}+Fe^{2+}+Mn^{2+}$. This is a consequence of relatively high SiO_2, and has been noted above.

(2) The proportion of the total Al that is in tetrahedral co-ordination is consequently low, and compares more closely with the values for pyroxenes from tholeiitic, high-alumina and calc-alkalic rocks than with those of the alkali types.

(3) In the diagrams of Al_z versus TiO_2 wt per cent and of Al_2O_3 wt per cent versus SiO_2 wt per cent, the pyroxenes plot in the field of the tholeiitic, high-alumina and calc-alkaline types.

The relations between oversaturated tholeiite, undersaturated tholeiite and critically undersaturated alkali basalts are illustrated by Yoder and Tilley (1962, p. 352). They point out that the norms of the pyroxenes from the alkali basalts studied by them contain nepheline, while the norms of the pyroxenes from the tholeiitic rocks contain considerable hypersthene or even quartz (p. 365, Table 5).

All the pyroxenes in the present study contain normative nepheline except 5 and 9B (Table 4); the amount of hypersthene in the norms of these two pyroxenes is small, and indicates only a very slight excess of silica over that required to satisfy the Na_2O for albite. Although normative hypersthene appears in 9B, the amount of nepheline in the norm of 9A ensures that the bulk pyroxene would also have nepheline in its norm. The absence of normative nepheline in pyroxene 5 is hardly surprising since the host rock, porphyritic banatite, contains about 60 wt per cent SiO_2, and about 5% of quartz appears in its norm.

Trend of Pyroxene Composition

The analyzed clinopyroxenes are plotted in Figs. 8 and 9 on the basis of atomic per cent Ca-Mg-Fe, where $Fe = Fe^{3+}+Fe^{2+}+Mn^{2+}$. Figure 8 shows the detailed relations of the various pyroxene fractions. The upper and lower limit of iron substitution occurs in pyroxenes 9B and 1 respectively. The trend of pyroxene compositions is from $Ca_{46.1}Mg_{40.8}Fe_{13.1}$ to

R. S. BOESEN

TABLE 4. C.I.P.W. NORMS OF ANALYSES IN TABLE 1

	1	2	3	4	5	6	7	8	9A	9B	10A	10	10B
Or	0.11	0.11	0.22	0.45	0.95	0.17	0.17	0.28	0.33	0.61	0.39	0.33	0.95
Ab	3.46	1.05	1.42	4.83	4.04	2.15	3.15	1.52	2.83	8.03	5.56	8.14	10.69
An	6.48	7.57	5.48	4.06	8.63	8.82	2.23	7.09	9.21	6.62	9.29	8.13	6.43
Ne	0.65	2.04	1.90	0.23	—	1.90	1.08	2.67	1.73	—	1.11	1.11	1.39
Di	81.85	81.17	83.32	79.97	75.44	80.55	89.58	81.07	76.53	71.94	75.46	73.84	71.34
Hyp	—	—	—	—	0.81	—	—	—	—	0.53	—	—	—
Ol	2.97	4.20	3.48	6.81	6.53	1.06	0.26	2.16	4.01	3.64	1.06	0.71	1.08
Il	1.00	1.33	0.91	0.85	1.08	1.38	0.46	1.23	1.20	3.92	1.79	1.56	1.46
Mt	3.47	2.45	3.25	2.57	2.69	4.17	2.64	3.91	4.12	4.72	4.96	5.79	6.19
Cm	0.02	0.11	0.13	0.02	0.09	—	—	0.07	0.02	—	0.02	—	—
Total	100.01	100.04	100.11	99.79	100.26	100.20	99.57	100.00	99.98	100.01	99.64	99.61	99.53

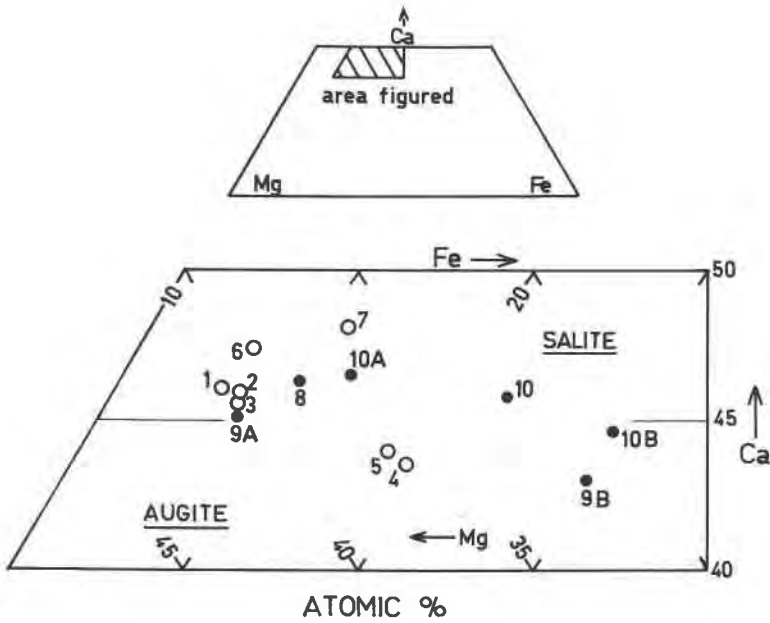Specimens numbered as in Table 1.

FIG. 8. Plot of analyses of the pyroxenes from the monzonitic complex on the conventional Ca-Mg-Fe atomic per cent diagram, where $Fe = Fe^{3+} + Fe^{2+} + Mn^{2+}$. Cross-hatched area in locality diagram is shown in detail immediately below. Solid circles represent analyses of pyroxenes from nepheline-bearing rocks. Numbers correspond to those of the analyses in Table 1.
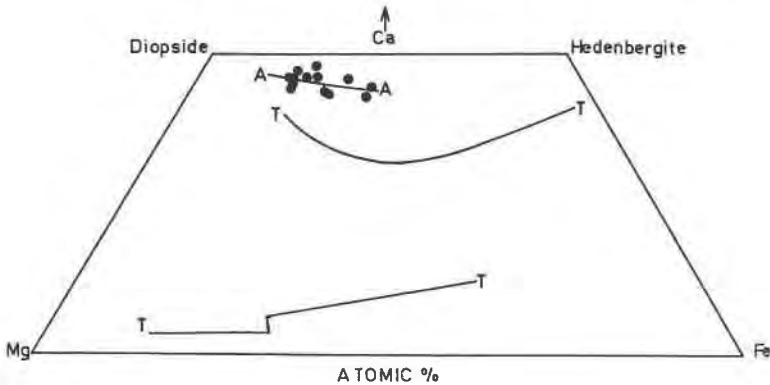

FIG. 9. Plot of analyses of the pyroxenes from the monzonitic complex on the conventional Ca-Mg-Fe atomic per cent diagram, where $Fe = Fe^{3+} + Fe^{2+} + Mn^{2+}$, together with the trend for pyroxenes of the alkali basalt magma (A—A) after Wilkinson (1956), and the tholeiitic Red Hill intrusion (T—T) after McDougall (1961).

$Ca_{43.0}Mg_{31.9}Fe_{25.1}$. The trends of zoning in the "ijolite" (9A, 9B) and the nepheline monzonite (10A, 10, 10B) are very similar to each other, and to the pyroxenite-banatite trend (2, 5 respectively). The plots of the three pyroxenes from the pyroxenitic rocks at Poole's Point (1, 2, 3) nearly coincide. The pyroxenes from the altered pyroxenite (6, 7) are more lime-rich than 1, 2 and 3, whereas 7, separated from the garnet-pyroxene rock, is noticeably poor in titania and alumina and rich in silica.

The pyroxenes from the monzonite and banatite (4, 5) plot very close to one another, slightly below the mid-point of the line joining the analyses of the core and rim of the "ijolite" pyroxene. The plots of 4 and 5 are curious in that they show that the pyroxene from the banatite is slightly more diopsidic than that from the more basic monzonite.

The trends for the pyroxenes from the tholeiitic intrusion at Red Hill (McDougall, 1961) and for those of the alkali basalt magma (Wilkinson, 1956) are compared in Fig. 9 with the pyroxenes studied herein.

PYROXENES IN OTHER MONZONITIC ROCKS

The analysis of a pyroxene from the Mt. Dromedary area given by Wilshire and Binns (1961, p. 198) has not been used in this study because the present writer was unable to determine either the exact location or the nature of the host rock.

Other examples of relatively potash-rich monzonitic intrusions emplaced in a late or post-orogenic environment occur at Port Cygnet, Tasmania; Milton, about 100 miles north of Mt. Dromedary; central Montana; the kentallenites of the South-West Highlands of Scotland; and possibly at the type locality for monzonite at Monzoni, in the Tyrol.

The pyroxene found in such intrusions is typically a lime-rich monoclinic variety. It is only rarely ophitic in form, and is colorless or pale green and very weakly pleochroic. In the highly alkalic rocks the pyroxene grains may have a deeper green rim or, more rarely, occur as aegirine-augite. Zoning by inclusions, color and birefringence is not uncommon (Hill and Kynaston, 1900, Plate XXIX; Larsen *et al.*, 1941). The striking constancy in composition of the pyroxenes from this type of association has been commented upon by Larsen *et al.* (1941), Pirsson (1905a) and others. Larsen *et al.* (1941), writing on the mineralogy of the igneous rocks of the Highwood Mountains, state (pp. 1843–1844) "the augites are pale green and characteristically zoned with recurrent zones of somewhat different color and extinction angle but with not much difference in composition . . . The augites show a remarkable uniformity in their optical properties in nearly all the rocks."

The analyses of the pyroxene from the shonkinite at Square Butte in

the Highwood Mountains district (Pirsson, 1905b, p. 98) and of that from the shonkinite at Mt. Dromedary are compared in Table 5.

The alkali basalt magma has a definite preponderance of soda over potash which is maintained in the strongly fractionated rocks, despite the

TABLE 5. ANALYSES OF PYROXENES FROM SHONKINITES

	8	A
SiO_2	50.14	49.42
TiO_2	0.65	0.55
Cr_2O_3	0.05	
Al_2O_3	3.90	4.28
Fe_2O_3	2.70	2.86
FeO	6.56	5.56
MnO	0.25	0.10
MgO	13.06	13.58
CaO	21.88	22.35
Na_2O	0.76	1.04
K_2O	0.05	0.38
P_2O_5	0.04	
H_2O	0.17	0.09
Total	100.21	100.21

Composition, atomic per cent

	8	A
Ca	46.3	46.9
Mg	38.5	39.6
[1]Fe	15.2	13.5

8: Pyroxene from shonkinite, Tilba Tilba (analyst R. S. Boesen).
A: Pyroxene from shonkinite, Square Butte (analyst L. V. Pirsson).
[1] $Fe = Fe^{3+} + Fe^{2+} + Mn^{2+}$.

fact that in the more felsic differentiates potash increases at a greater rate than soda. The igneous rocks at Mt. Dromedary, on the other hand, have a preponderance of potash over soda in all but the ultramafic types, and there is a trend towards relative enrichment in potash. This difference in potash-soda relationship between the alkali basalts and the monzonitic suite is reflected in the pyroxenes. The soda content of the pyroxenes from monzonitic and syenitic rocks derived from alkali basalt (Yagi, 1953) is greater than that of the pyroxenes from comparable rocks at Mt. Dromedary and similar occurrences.

CONCLUSIONS

The pyroxenes of the monzonitic complex at Mt. Dromedary and of some other similar occurrences are lime-rich monoclinic varieties with a range of composition similar to that proposed for pyroxenes of the alkali basalt magma. They can be distinguished chemically from the alkali basalt pyroxenes by their slightly higher content of silica and lower titania, soda and perhaps alumina. In thin section they are usually pale green, weakly pleochroic, and fairly euhedral, whereas the pyroxenes of the alkali basalt type are most often pink or mauve, distinctly pleochroic, and commonly ophitic. The pyroxenes of the felsic differentiates of alkali basalt magma appear to be more sodic than their counterparts in the monzonitic complex at Mt. Dromedary.

It is suggested that the relatively small differences between the two groups of pyroxenes is related to the trends of fractionation of the parent magmas, with $Na_2O > K_2O$ in the alkali basalts, and $K_2O > Na_2O$ in the monzonitic suite.

ACKNOWLEDGMENTS

REFERENCES

BERMAN, H. (1937) Constitution and classification of natural silicates. *Am. Mineral.* **22,** 331–415.

BROWN, G. M. (1957) Pyroxenes from the early and middle stages of fractionation of the Skaergaard intrusion, East Greenland. *Mineral. Mag.* **31,** 511–543.

——— AND E. A. (1963) Pyroxenes from the late stages of fractionation of the Skaergaard intrusion, East Greenland. *Jour. Petrology*, **4,** 175–197.

BROWN, I. A. (1930) The geology of the South Coast of New South Wales. iii. The monzonitic complex of the Mount Dromedary district. *Proc. Linn. Soc. New South Wales* **55,** 637–698.

——— (1933) The geology of the South Coast of New South Wales, with special reference to the origin and relationships of the igneous rocks. *Proc. Linn. Soc. New South Wales,* **58,** 334–362.

CHALLIS, G. A. (1963) Layered xenoliths in a dyke, Awatere Valley, New Zealand. *Geol. Mag.* **100,** 11–16.

EVERNDEN, J. F. AND J. R. RICHARDS (1962) Potassium-argon ages in eastern Australia. *Jour. geol. Soc. Austral.* **9,** 1–50.

HALLIMOND, A. F. (1950), Universal stage methods. *Mining Mag.* **83,** 12–22.

HESS, H. H. (1949) Chemical composition and optical properties of common clinopyroxenes Part 1. *Am. Mineral.* **34,** 621–666.

—— (1960) Stillwater igneous complex, Montana. *Geol. Soc. Am. Mem.* **80.**

HILL, J. B. AND H. KYNASTON (1900) On kentallenite and its relations to other igneous rocks in Argyllshire. *Quart. Jour. Geol. Soc. London*, **56**, 531–557.

KUNO, H. (1955) Ion substitution in the diopside-ferropigeonite series of clinopyroxenes. *Am. Mineral.* **40**, 70–93.

—— AND M. SAWATARI (1934) On the augites from Wadaki, Idu, and from Yoneyama, Etigo, Japan. *Jap. Jour. Geol. Geogr.* **11**, 327–343.

KUSHIRO, I. (1960) Si-Al relations in clinopyroxenes from igneous rocks. *Bull. Geol. Soc. Am.* **64**, 769–810.

LARSEN, E. S., C. S. HURLBUT, JR., B. F. BUIE AND C. H. BURGESS (1941) Igneous rocks of the Highwood Mountains, Montana. Part VI. Mineralogy. *Bull. Geol. Soc. Am.* **52**, 1841–1856.

LE BAS, M. J. (1962) The role of aluminium in igneous clinopyroxenes with relation to their parentage. *Am. Jour. Sci.* **260**, 267–288.

McDOUGALL, I. (1961) Optical and chemical studies of pyroxenes in a differentiated Tasmanian doler'te. *Am. Mineral.* **46**, 661–687.

MUIR, I. D. (1951) The clinopyroxenes of the Skaergaard intrusion, eastern Greenland. *Mineral. Mag.* **29**, 690–714.

MURRAY, R. J. (1954) The clinopyroxenes of the Garbh Eilean sill, Shiant Isles. *Geol. Mag.* **91**, 17–31.

PEACOCK, M. A. (1931) Classification of igneous rocks. *Jour. Geol.* **39**, 54–67.

PIRSSON, L. V. (1905a) The petrographic province of Central Montana. *Am. Jour. Sci.* **170**, 35–49.

—— (1905b) Igneous rocks of the Highwood Mountains, Montana. *Bull. U. S. Geol. Surv.* **237.**

SEGNIT, E. R. (1953) Some data on synthetic aluminous and other pyroxenes. *Mineral. Mag.* **30**, 218–226.

TILLEY, C. E. (1950) Some aspects of magmatic evolution. *Quart. Jour. Geol. Soc. London*, **106**, 37–61.

WARREN, B. E. AND J. BRISCOE (1931) The crystal structure of the monoclinic pyroxenes. *Zeit. Krist.* **80**, 391–401.

WILKINSON, J. F. G. (1956) Clinopyroxenes of alkali olivine-basalt magma. *Am. Mineral.* **41**, 724–743.

—— (1957) The clinopyroxenes of a differentiated teschenite sill near Gunnedah, New South Wales. *Am. Jour. Sci.* **256**, 1–39.

—— (1958) The petrology of a differentiated teschenite sill near Gunnedah, New South Wales. *Am. Jour. Sci.* **256**, 1–39.

WILSHIRE, H. G. AND R. A. BINNS (1961) Basic and ultrabasic xenoliths from volcanic rocks of New South Wales. *Jour. Petrology* **2**, 185–208.

YAGI, K. (1953) Petrochemical studies on the alkaline rocks of the Morotu district, Sakhalin. *Bull. Geol. Soc. Am.* **64**, 769–810.

YODER, H. S., JR. AND C. E. TILLEY (1962) Origin of basalt magmas: An experimental study of natural and synthetic rock systems. *Jour. Petrology*, **3**, 342–532.